Near-field radiative heat transfer in many-body systems

Philippe Ben-Abdallah

Laboratoire Charles Fabry, Institut d'Optique, Paris, France

pba@institutoptique.fr

KITP-Lecture4-Quantum and Thermal Electrodynamic Fluctuations in the Presence of Matter: Progress and Challenges

Heat transfer in far field

Kirchoff 1862
(Radiometry)

Planck 1901
(blackbody theory)

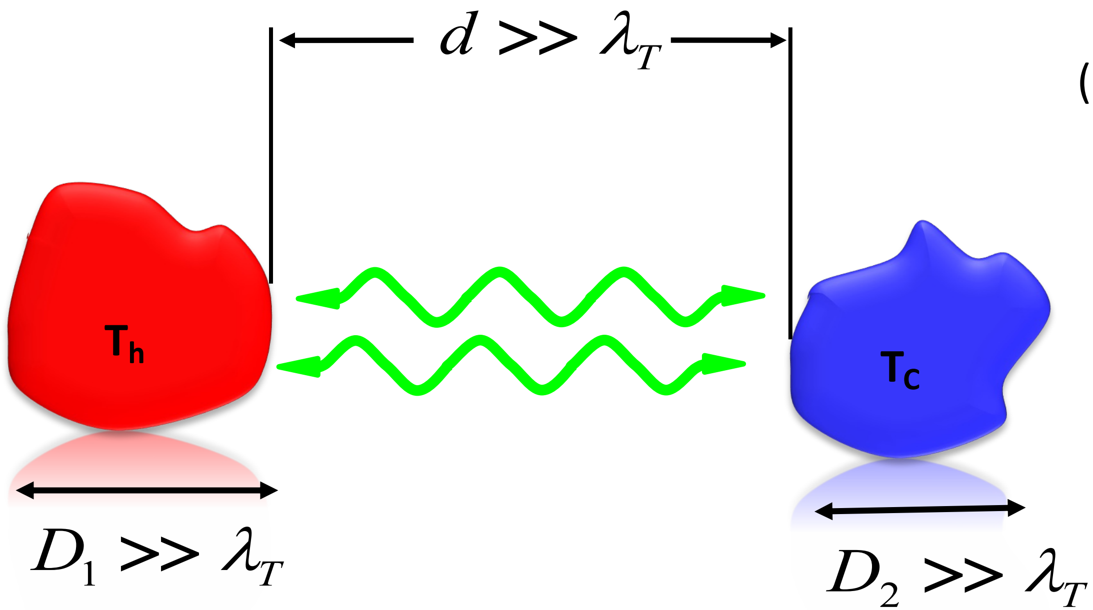

$$\phi < \underbrace{\sigma(T_h^4 - T_c^4)}_{\text{Heat transfer between two blackbody}}$$ **Stefan-Boltzmann limit**

Heat transfer in near-field

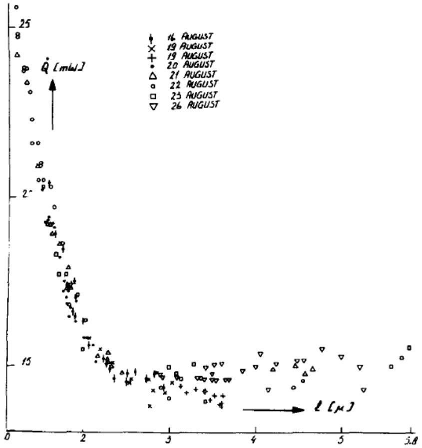

Hargreaves
1969 experiment

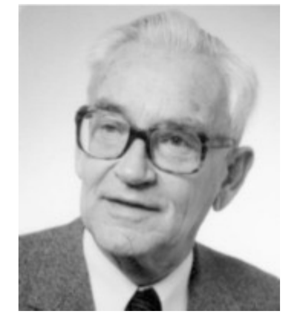

Polder & Van Hove,
1971 theory

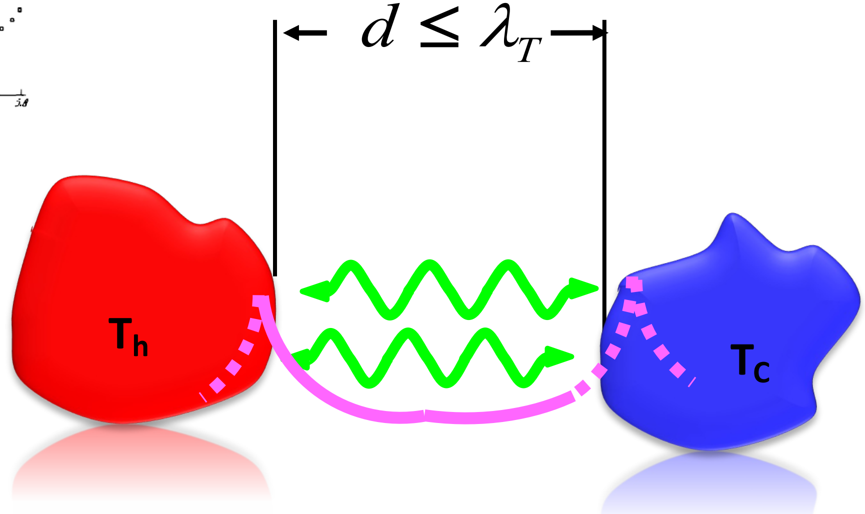

$$\phi > \sigma(T_h^4 - T_c^4)$$

Tunneling of non-propagative photons

Since then, more than 20 experimental proofs:

PRL,95, 224301, 2005; PRB, 78, 115303, 2008; APL 92, 133106, 2008; Nano Lett. 9, 2909 , 2009; Nature Photon. 3, 514, 2009; PRL 107, 014301, 2011; Rev. Sci. Instrum. 82, 055106 , 2011; PRL 109, 224302, 2012; PRL, 108, 234301, 2012; PRL 109, 264301, 2012; Nature Nano. 10, 253, 2015; Nature 528, 387, 2015; Nature Nano. 11, 515, 2016; APL, 109, 203112, 2016; Nat. Commun. 8, 14475, 2017, PRL , 120, 175901 (2018)…

Many-body near-field heat transfer

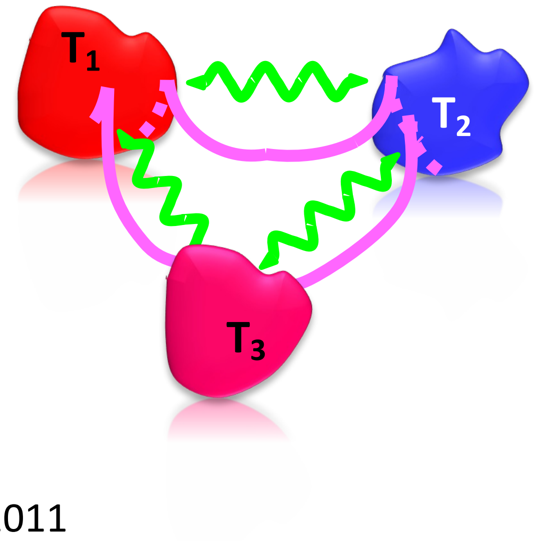

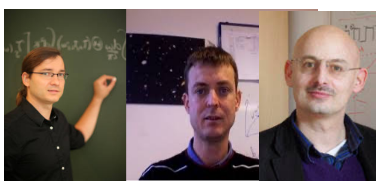

dipoles 2011

 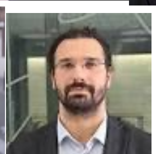 … 

3 body 2014

  … 

N body 2017

<u>Many body effects</u>:

-non additivity of flux

-anomalous heat transport regimes

-photon tunneling amplification

-multistable states

…

-open the door to new functionalities

<u>Review</u>:

Biehs et al. Rev. Mod. Phys., 93, 025009 (2021)

Latella et al., Opt. Express, 29 (16) , 24816 (2021)

Heat transfer in many-body systems

Energy balance (neglecting the background contribution)

$$\frac{dT_i}{dt} = \sum_{j \neq i} \wp_{j \to i}(T_1, \ldots, T_N)$$

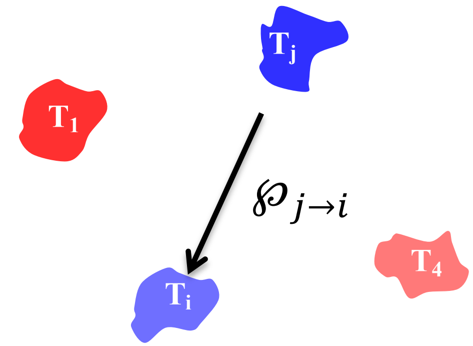

Using the Landauer formalism

$$\wp_{j \to i} = \int_0^\infty [\theta(T_j, \omega)\mathfrak{I}_{ji}(\omega) - \theta(T_i, \omega)\mathfrak{I}_{ij}(\omega)] \frac{d\omega}{2\pi}$$

with the transmission coefficient (arbitrary non-reciprocal materials)

$$\mathfrak{I}_{ji}(\omega) = \frac{4}{3}\left(\frac{\omega}{c}\right)^4 Im\, Tr\left[\boldsymbol{\alpha}_i \mathscr{G}_{\boldsymbol{ij}} \frac{\boldsymbol{\alpha}_j - \boldsymbol{\alpha}_j^\dagger}{\boldsymbol{2i}} \mathscr{G}_{\boldsymbol{ij}}^\dagger\right]$$ (small objects)

Polarizability tensor   Full Green (multiscattering)

PRL **107**, 114301(2011), RMP **93**, 025009 (2021)

Outline

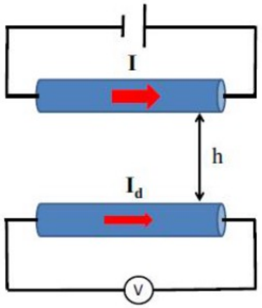

- Thermal photon-drag

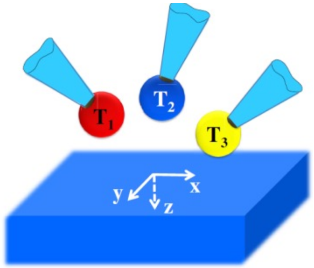

- Many-body heat flux focusing

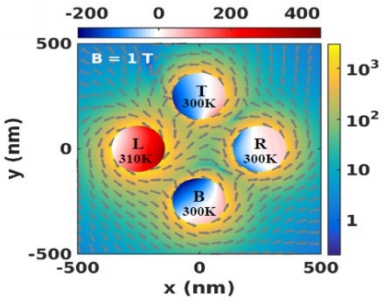

- Thermomagnetic control of near-field heat exchanges

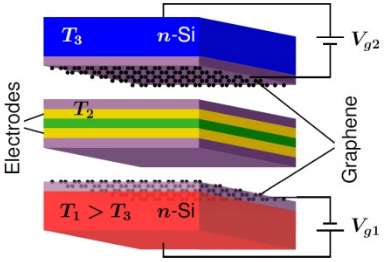

- Pyroelectric near-field energy conversion

Thermal photon-drag

Coulomb drag

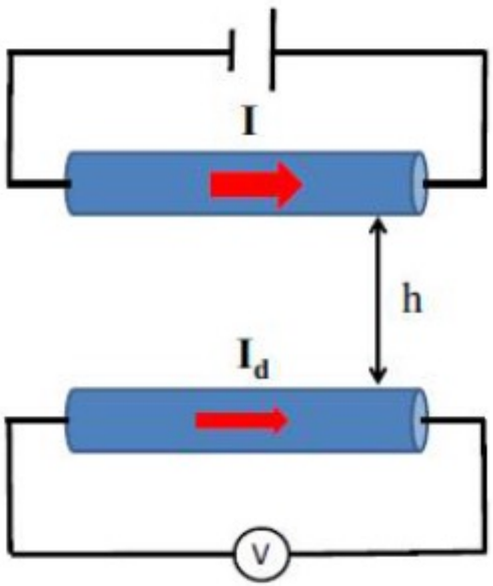

Active circuit

h~range of Coulombic interactions

Passive (open) circuit

Induced voltage

<u>Drag resistance</u>: $$R_D = \frac{V}{I}$$

Primary current

M. B. Pogrebinskii, Sov. Phys. Semicond. **11**, 372 (1977).

Thermal photon drag

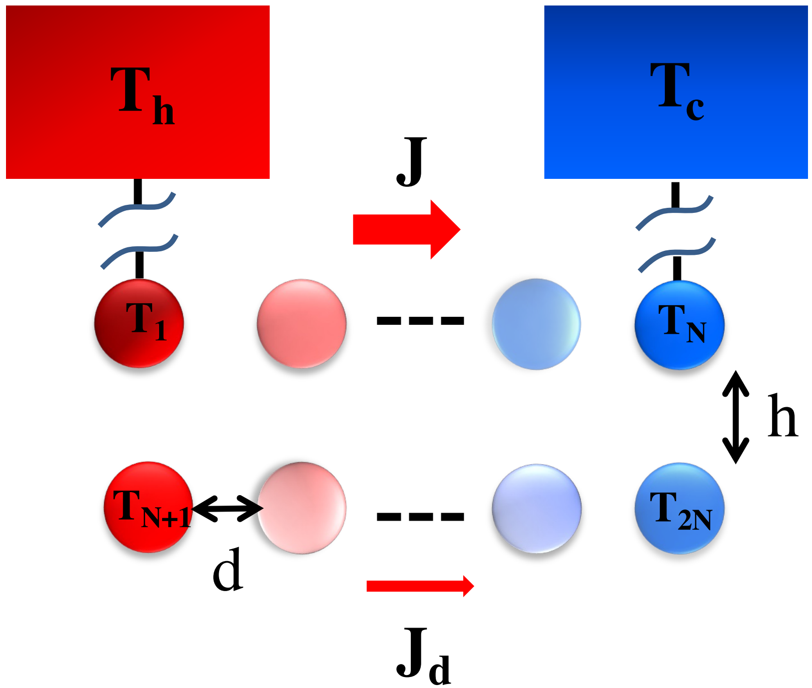

In steady state regime:

$$\begin{cases} \phi_{th,i} + \sum_{j\neq i}^{2N} \varphi_{j\to i}(T_1, \dots, T_{2N}) = 0 \quad (i = 1, N) \\ \sum_{\substack{j\neq i \\ j\neq 1,N}}^{2N} \varphi_{j\to i}(T_1, \dots, T_{2N}) = 0 \quad (i \neq 1,N) \end{cases}$$

$(T_1, \dots, T_{2N})$ Equilibrium state

Drag thermal resistance:

$V \leftrightarrow \Delta T, I \leftrightarrow J$ $\longrightarrow$ $R_D = \dfrac{\Delta T}{J}$

Phys. Rev. B **99**, 201406(R) (2019)

Controlling the local temperature gradient

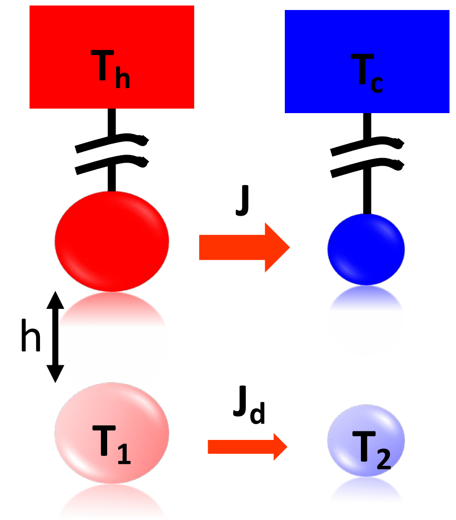

¨Positive drag

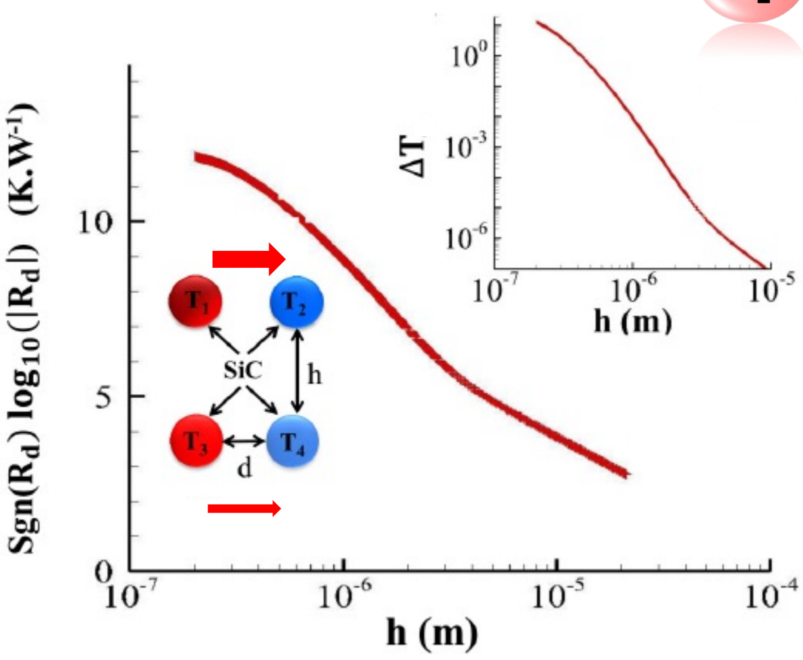

Negative drag

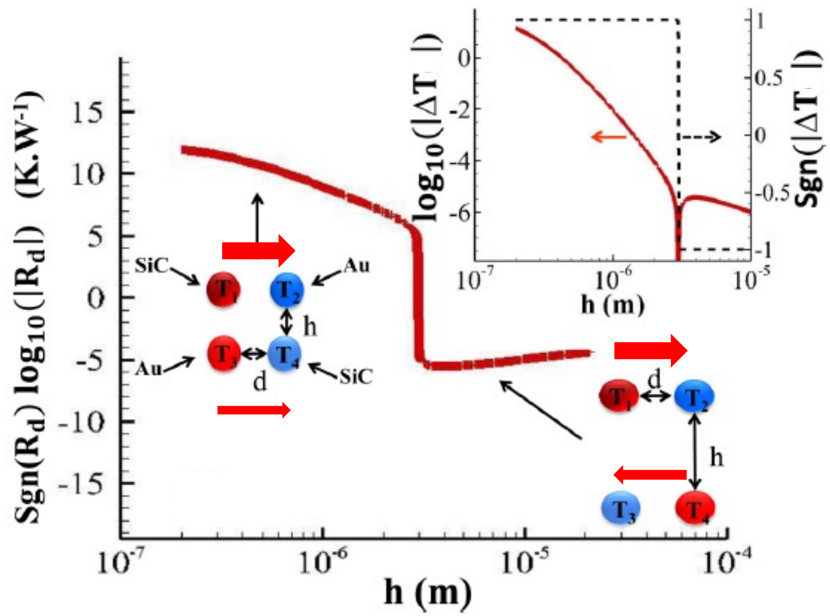

Phys. Rev. B **99**, 201406(R) (2019)

Many-body heat focusing

Local heating and magnetic-recording

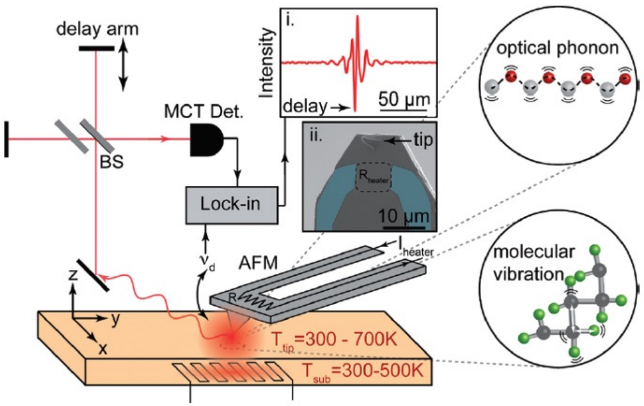

Jones and Raschke
Nano Lett. 12, 1475 (2012)

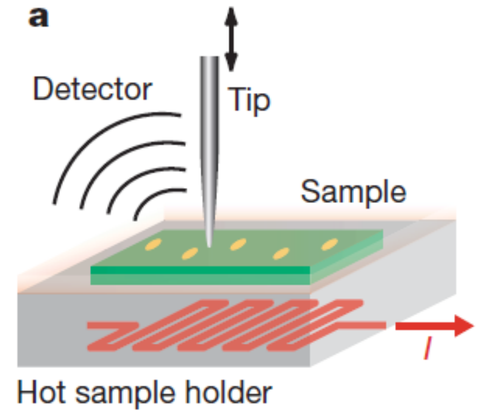

De Wilde et al.
Nature 444, 740 (2006)

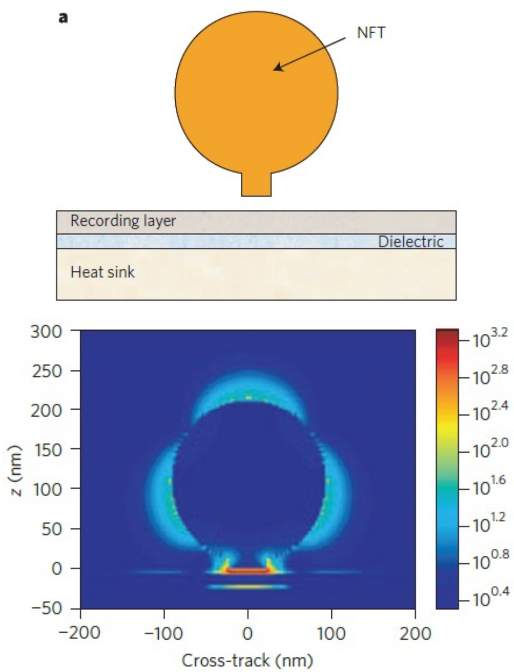

Challener et al.,
Nat. Phot. 3, 220 (2009)

Spatial control of Poynting vector

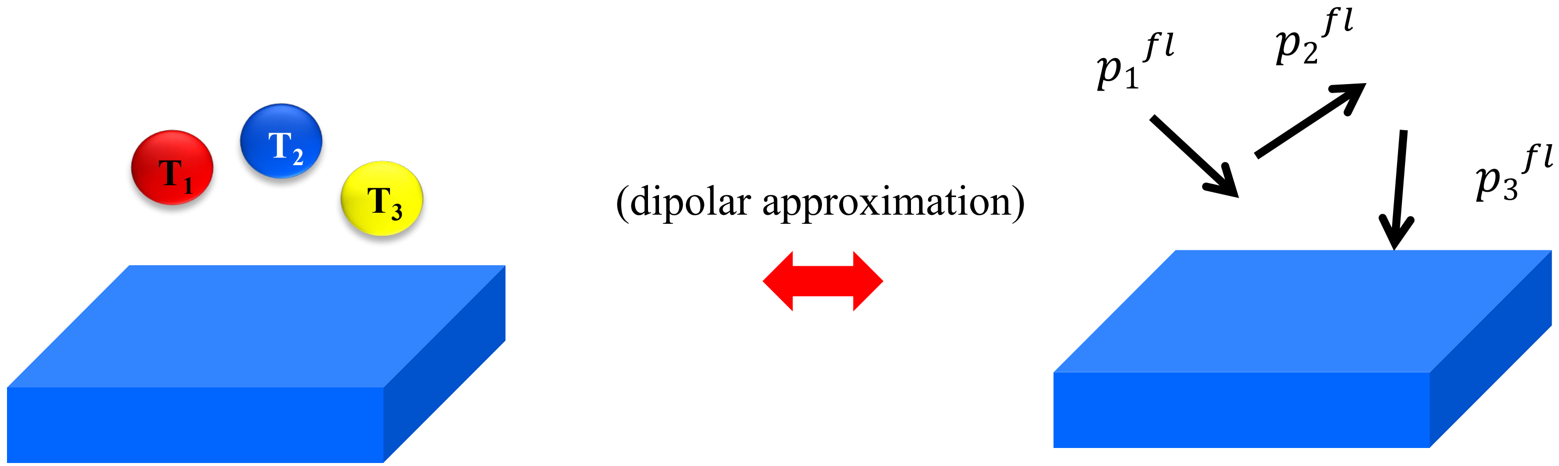

$$\boldsymbol{E}(\boldsymbol{r},\omega) = \omega^2 \mu_0 \sum_{i=1}^{N} \boldsymbol{g}\,(\boldsymbol{r},\boldsymbol{r}_i)\,\boldsymbol{p}_i^{\,fl} + scattered\ bath$$

$$\langle S_j(\boldsymbol{r},\omega)\rangle = \frac{\omega^2}{c^2}\sum_{i=1}^{N} a_j\,(\boldsymbol{r},\boldsymbol{r}_i,\omega)\theta(T_i,\omega)$$

Scattering

Temperature dependent weighting

PRL, 123, 264301 (2019)

Multitip Near-Field Scanning Thermal Microscopy

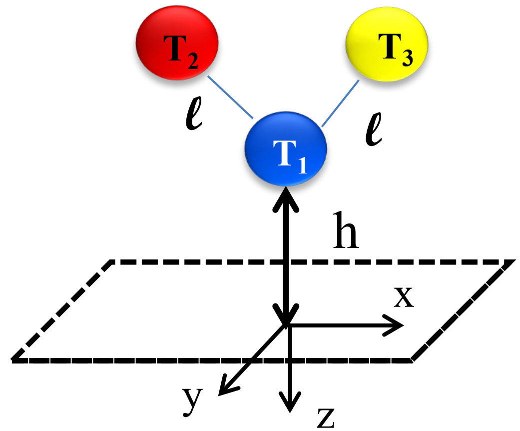

PRL, 123, 264301 (2019)

$T_1=T_2=T_3=300$ K

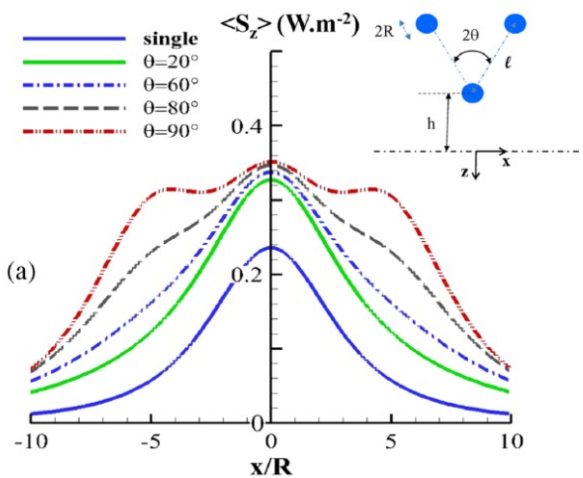

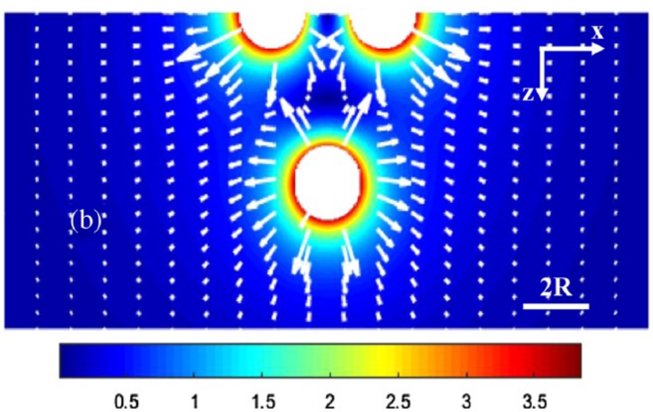

$T_2=T_3=350$ K $T_1=300$ K

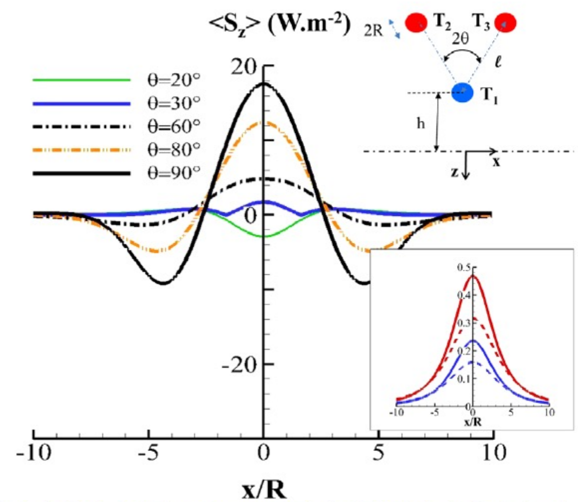

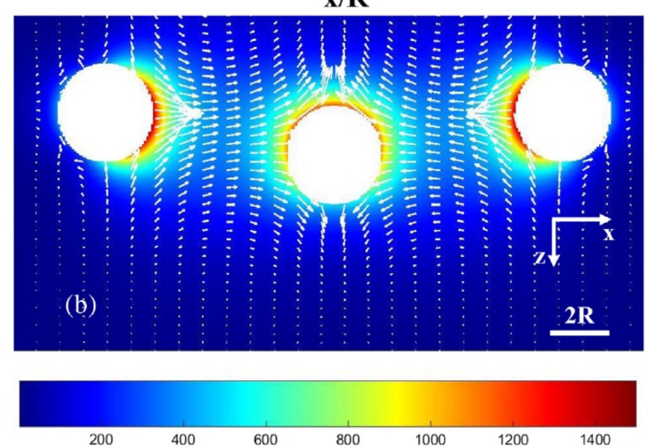

$h=4R$, $\ell=5R$, $R=20$ nm

$T_{single}=350$ K

Multitip Near-Field Scanning Thermal Microscopy

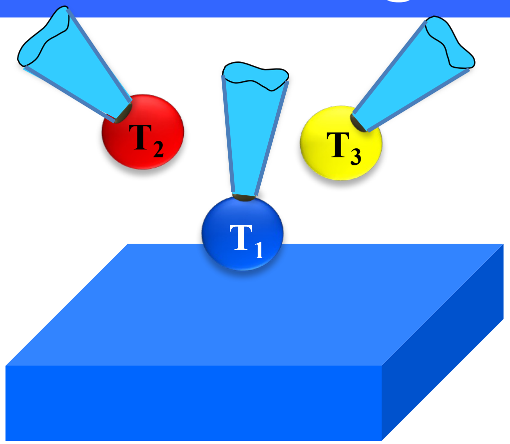

$T_2=T_3=350$ K $\quad T_1=300$ K

(non-emitting substrate)

$\theta = 80°$, $T_{single}=350$ K

x=0, y=0

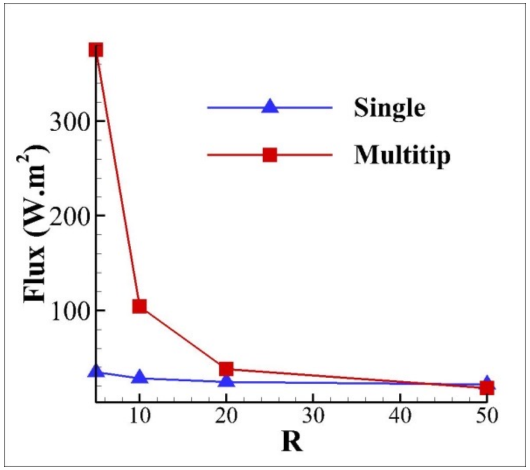

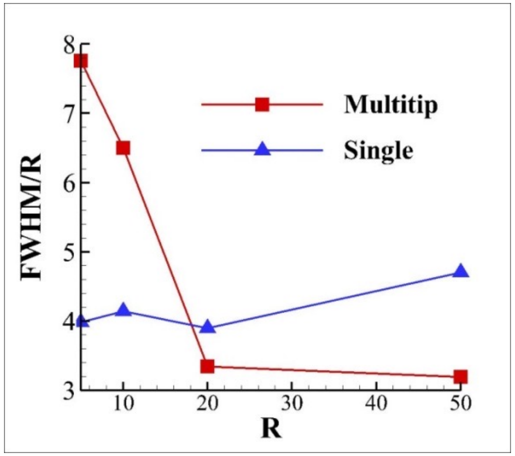

Amplification (>×8 single)

Focalisation much beyond the diffraction limit

Potential applications: heat assisted recording, nanoscale IR spectroscopy, thermal properties measurement…

PRL, 123, 264301 (2019)

Thermomagnetic control of near-field heat exchanges

Non-Hermitian many-body systems

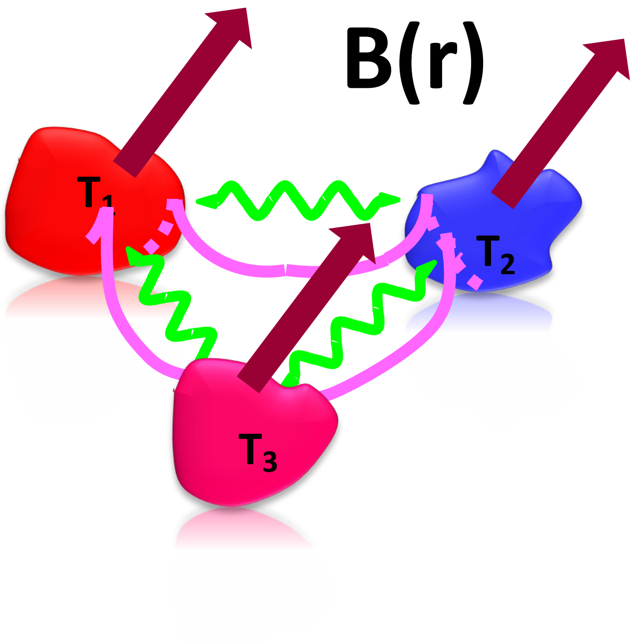

Energy balance close to equilibrium

$$\partial_t \boldsymbol{T} = \widehat{\boldsymbol{G}}(\boldsymbol{B})\boldsymbol{T}$$

temperatures

$$\boldsymbol{T} = \begin{pmatrix} T_1 \\ T_2 \\ T_3 \end{pmatrix}$$

conductances

$$\widehat{\boldsymbol{G}} = \begin{pmatrix} -\sum_{j\neq 1} G_{1j} & G_{12} & G_{13} \\ G_{21} & -\sum_{j\neq 2} G_{2j} & G_{23} \\ G_{31} & G_{32} & -\sum_{j\neq 3} G_{3j} \end{pmatrix}$$

$\widehat{\boldsymbol{G}}(\boldsymbol{B})$ is real and non symmetric

Heat transfers in many body systems under the action of an external field as some analogies with the evolution of a quantum non-Hermitian system

Classical Hall effect and thermal Hall effect

Edwin Hall,1879

Lorentz Force:

$F = q[E + (v \times B)]$

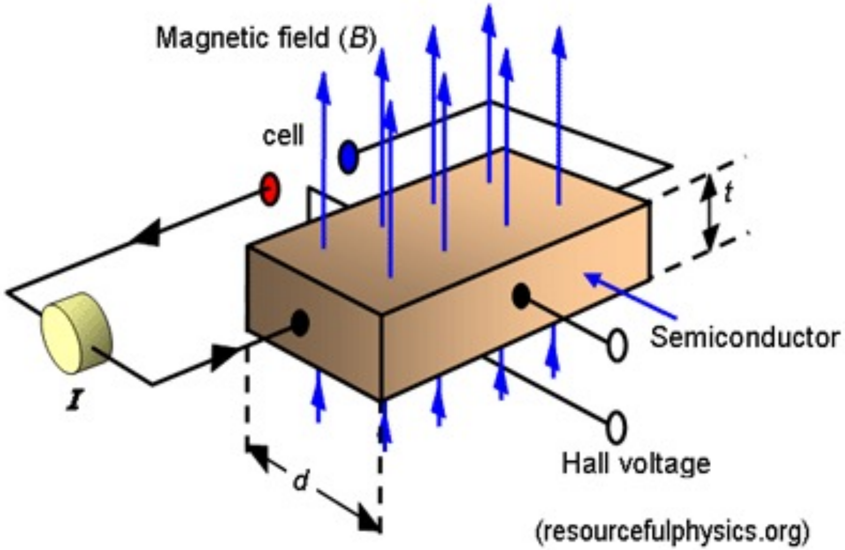

(resourcefulphysics.org)

Righi,Leduc,1888

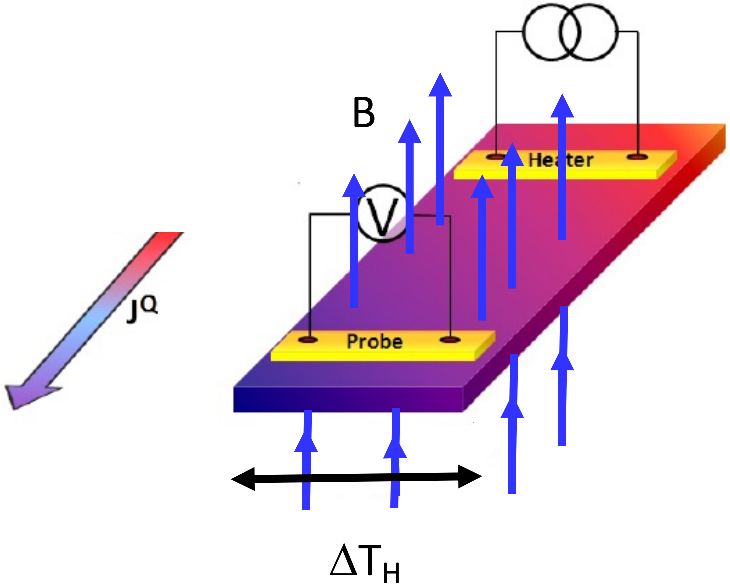

Strohm, 2005 (phonon Hall effect)

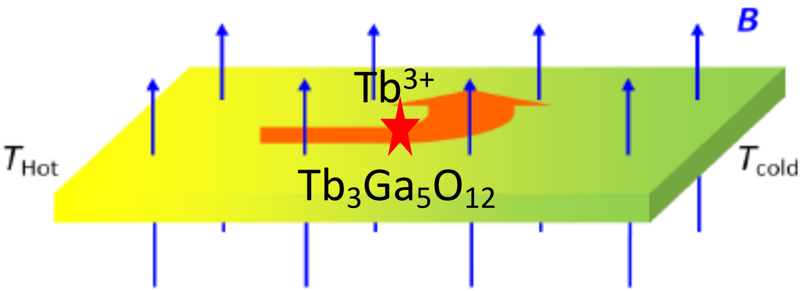

Mori et al., PRL, 113, 265901 (2014)

Photon thermal Hall effect

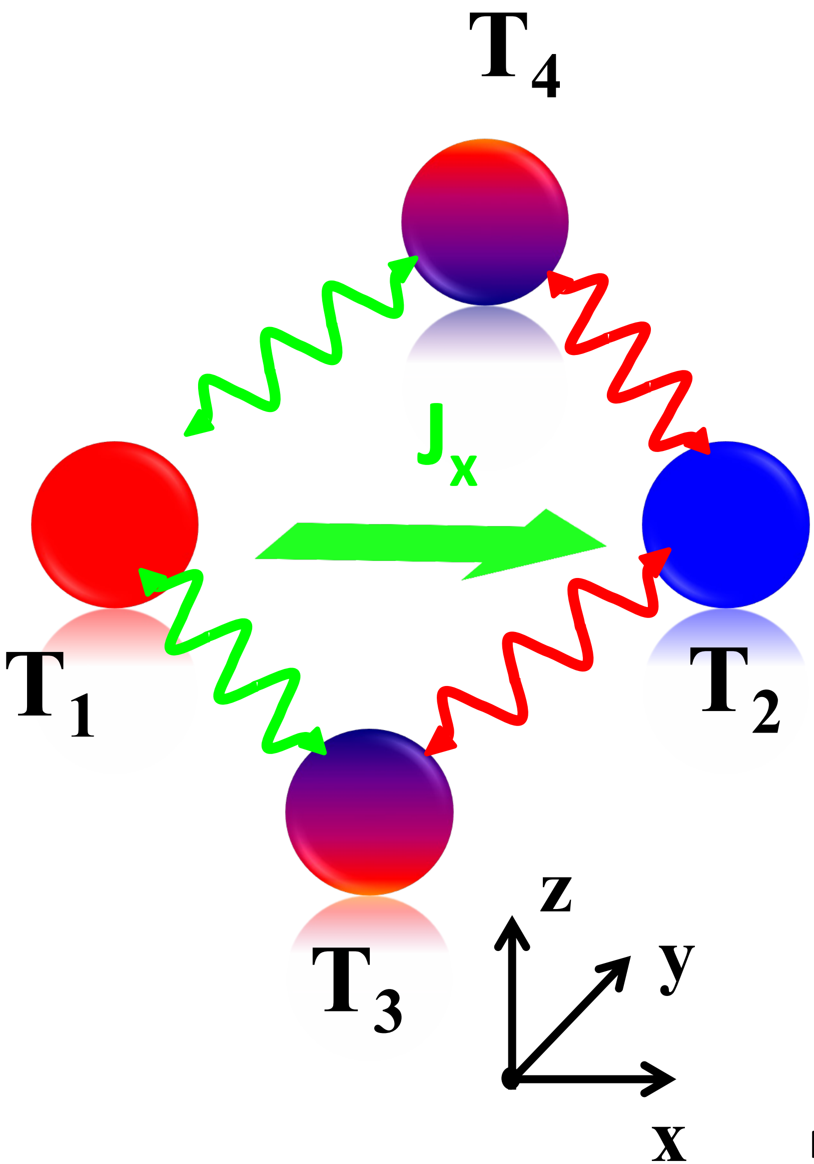

4-terminal InSb (magneto-optical) junction

B=0 ➡ $\varepsilon_{InSb} = \begin{pmatrix} \varepsilon_1 & 0 & 0 \\ 0 & \varepsilon_1 & 0 \\ 0 & 0 & \varepsilon_1 \end{pmatrix}$

$\varepsilon_1(B) = \varepsilon_\infty \left(1 + \frac{\omega_L^2 - \omega_T^2}{\omega_T^2 - \omega^2 - i\Gamma\omega} + \frac{\omega_p^2(\omega + i\gamma)}{\omega[\omega_c^2 - (\omega + i\gamma)^2]}\right)$

with $\omega_c = \frac{eB}{m^*}$ cyclotron frequency

T_3=T_4 ➡ **J_H=J_y=0**

No Hall flux

PRL 116, 084301 (2016)

Photon thermal Hall effect

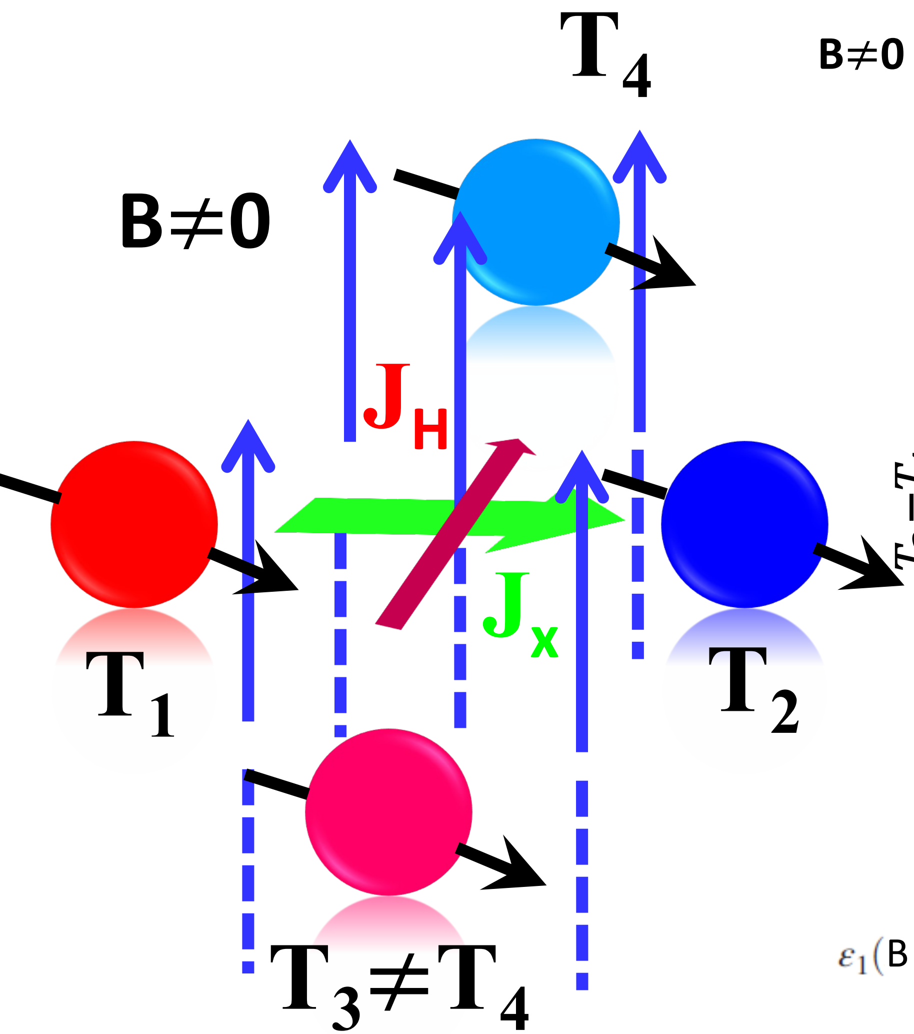

$$\varepsilon = \begin{pmatrix} \varepsilon_1 & -i\varepsilon_2 & 0 \\ i\varepsilon_2 & \varepsilon_1 & 0 \\ 0 & 0 & \varepsilon_3 \end{pmatrix}$$

B≠0 → InSb anisotropic (symmetry breaking) → **$J_H \neq 0$**

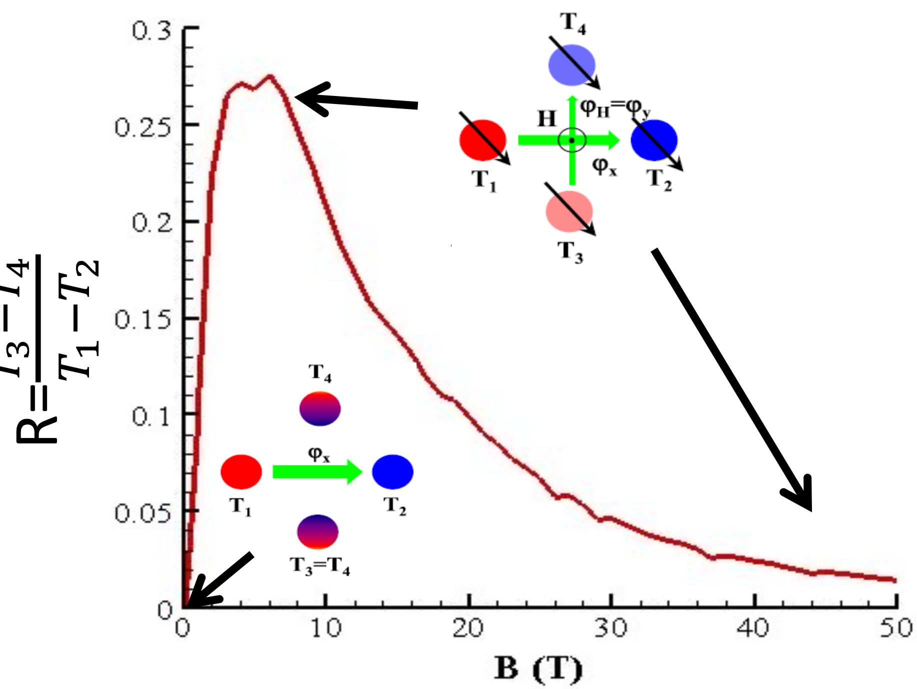

$$\varepsilon_1(\mathrm{B}) = \varepsilon_\infty\left(1 + \frac{\omega_L^2 - \omega_T^2}{\omega_T^2 - \omega^2 - i\Gamma\omega} + \frac{\omega_p^2(\omega + i\gamma)}{\omega[\omega_c^2 - (\omega + i\gamma)^2]}\right)$$

$$\varepsilon_2(\mathrm{B}) = \frac{\varepsilon_\infty\omega_p^2\omega_c}{\omega[(\omega + i\gamma)^2 - \omega_c^2]}$$

$$\varepsilon_3 = \varepsilon_\infty\left(1 + \frac{\omega_L^2 - \omega_T^2}{\omega_T^2 - \omega^2 - i\Gamma\omega} - \frac{\omega_p^2}{\omega(\omega + i\gamma)}\right)$$

Photon thermal Hall effect

Local resonances :

$$\mathrm{Det}[\,(\bar{\bar{\varepsilon}} - \varepsilon_h \bar{\bar{1}})(\bar{\bar{\varepsilon}} + 2\varepsilon_h \bar{\bar{1}})]=0 \quad \begin{cases} \varepsilon_3(\omega) + 2\varepsilon_h = 0 & (m=0) \\ [\varepsilon_1(\omega) + 2\varepsilon_h] \pm \varepsilon_2(\omega) = 0 & (m=\pm 1) \end{cases}$$

Flux lines:

$$\langle \vec{S} \rangle = \int_0^\infty \frac{d\omega}{2\pi} 2\mathrm{Re}\langle(\vec{E}_\omega \times \vec{H}^*_\omega)\rangle$$

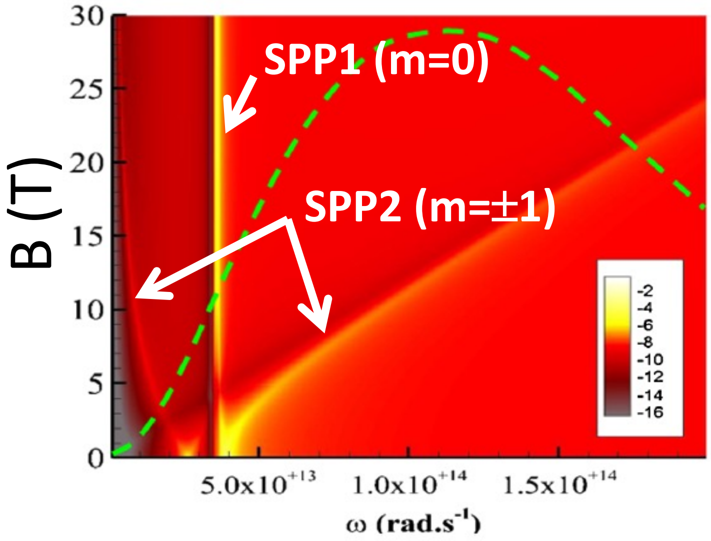

Dispersion of resonant modes

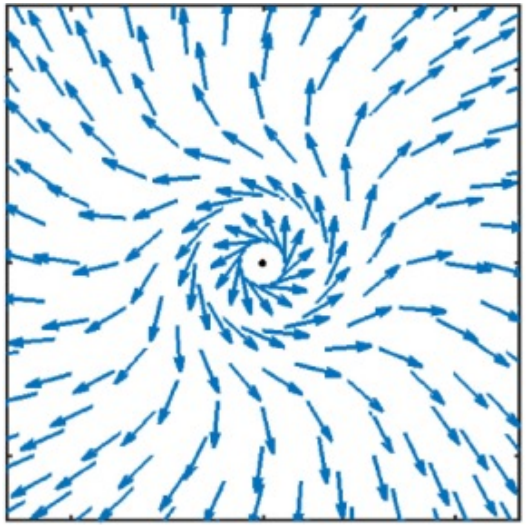

Vortex-like flux lines

PRL 116, 084301 (2016)

PRB **97**, 205414 (2018)

Photon thermal Hall effect

B=0

B=1 T

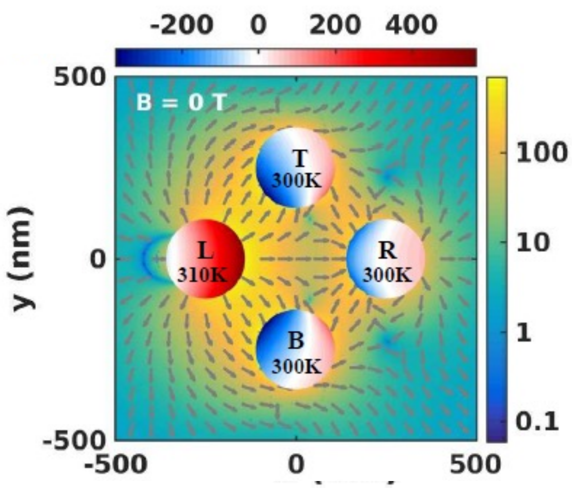

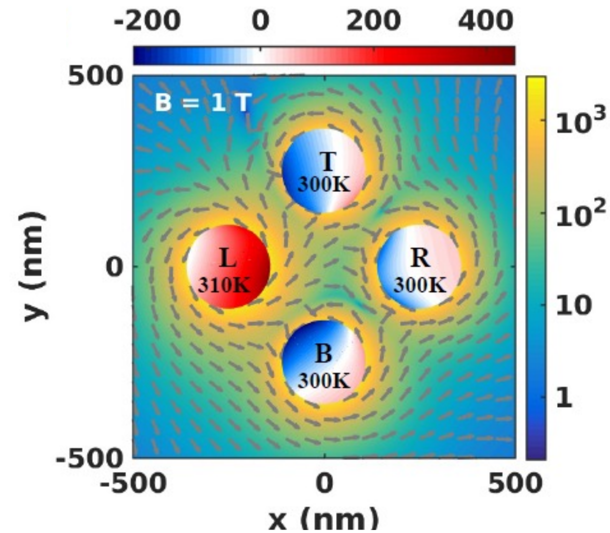

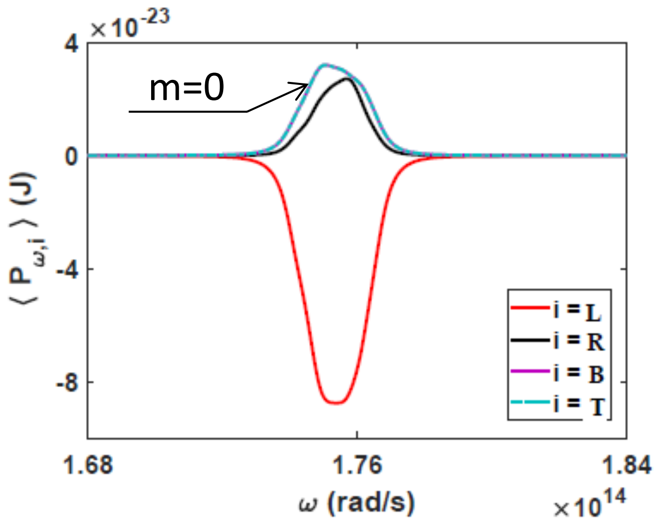

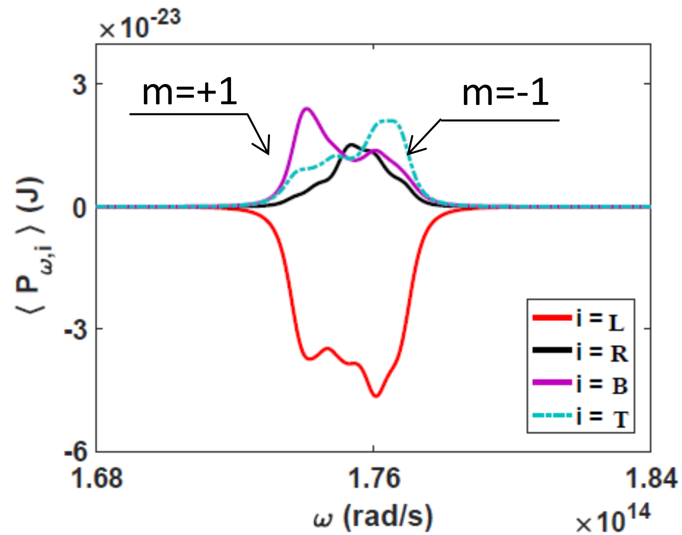

J. of Photonics for Energy, 032711 (2019)

Near-field pyroelectric conversion

Pyroelectric effect

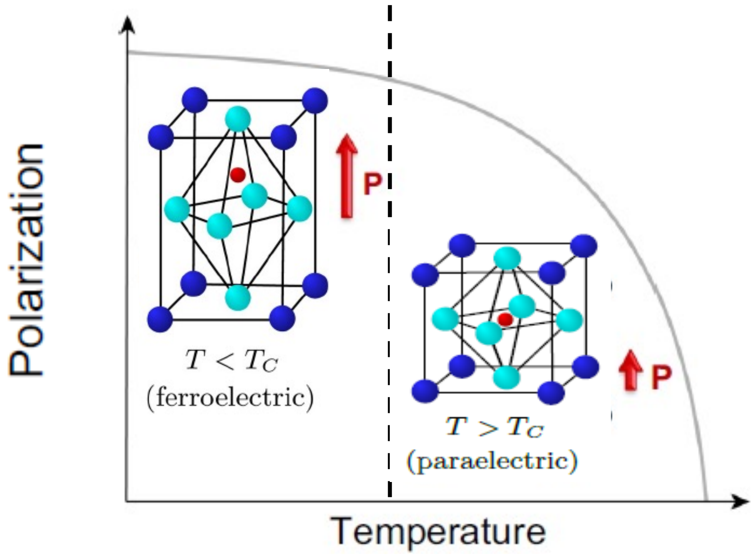

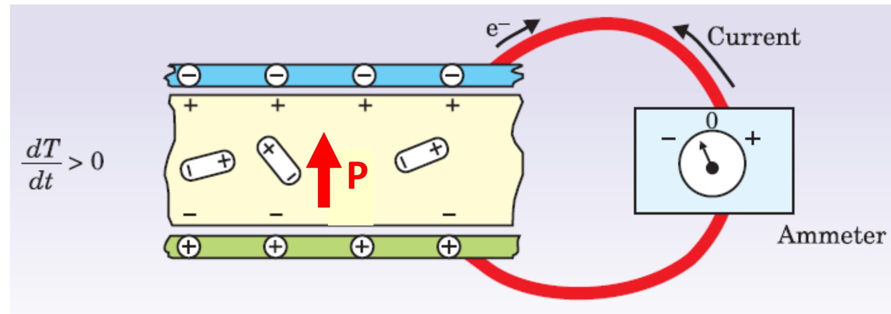

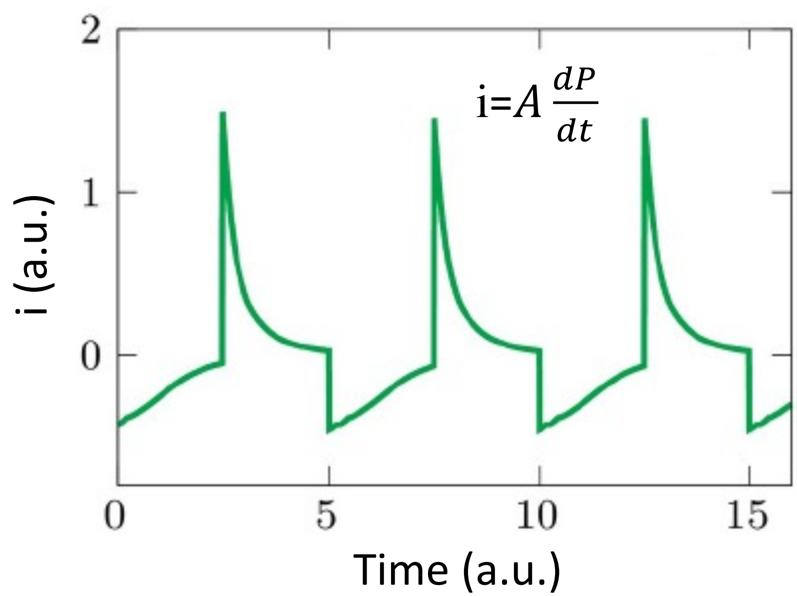

Pyroelectric conversion driven by graphene-based FET

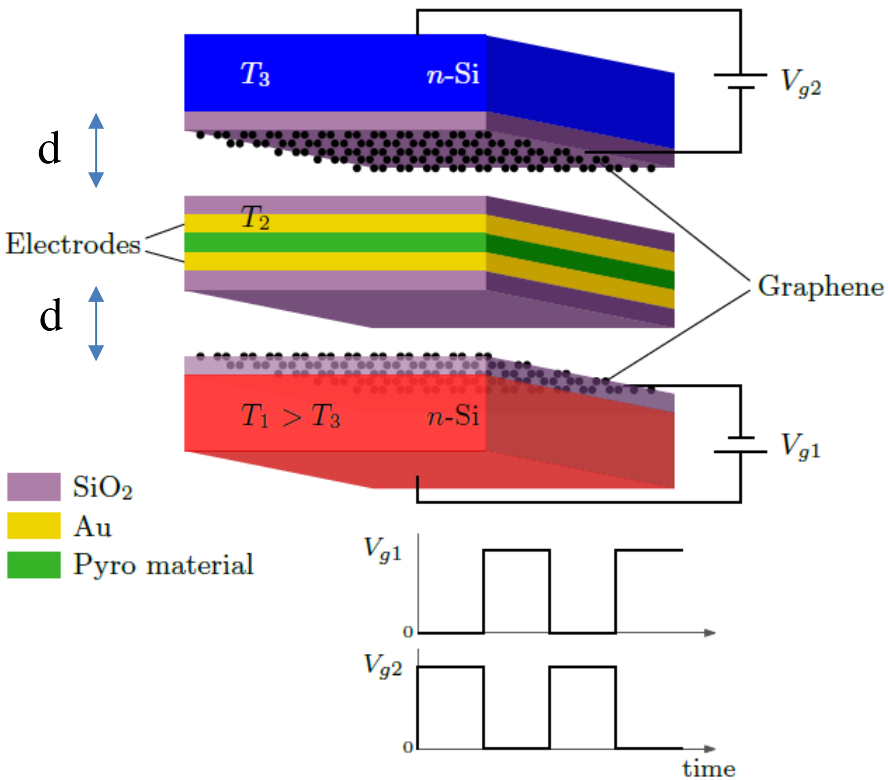

Graphene field-effect transistor:

$$n_{gi} = C_g V_{gi}/e$$

$$C_g = \varepsilon_g/\delta_g$$

$$\mu_{gi} = \hbar v_F \sqrt{\pi n_{gi}}$$

Novoselov et al. Science (2004)

d=20 nm; f~kHz

T_1=400 K; T_3=300 K

δ_g=5 nm

Sci. Rep., 11:19489 (2021)

Operating mode of converter

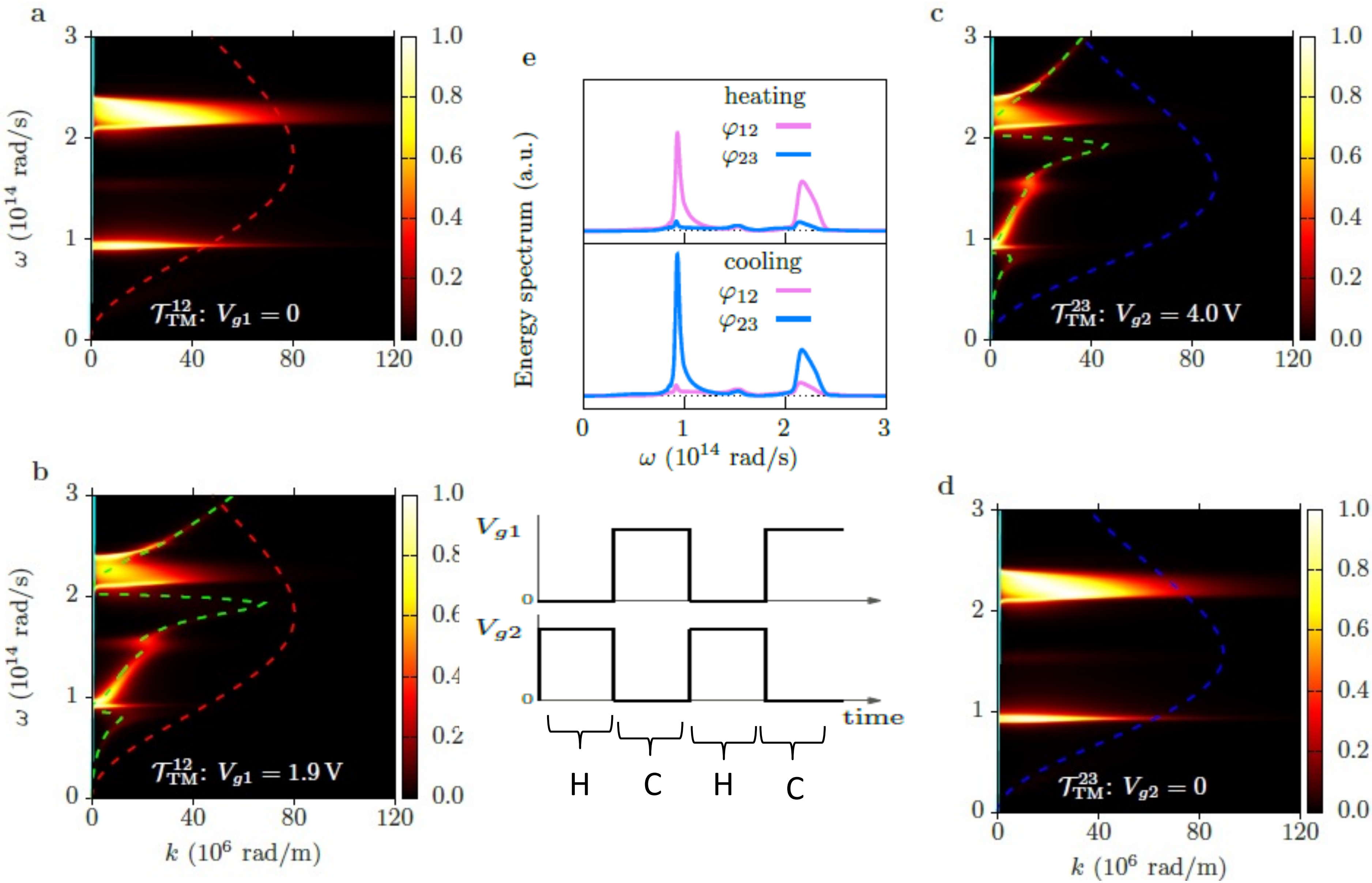

Pyroelectric conversion driven by graphene-based FET

$V_{g1}=V_{g2}=1$ V

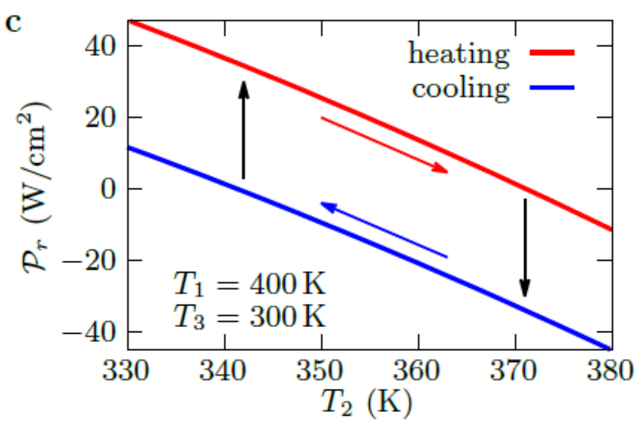

$$\mathcal{P}_r(V_{gi};T_2,t) = \int_0^\infty \frac{d\omega}{2\pi}\varphi_{12}(\omega) - \int_0^\infty \frac{d\omega}{2\pi}\varphi_{23}(\omega)$$

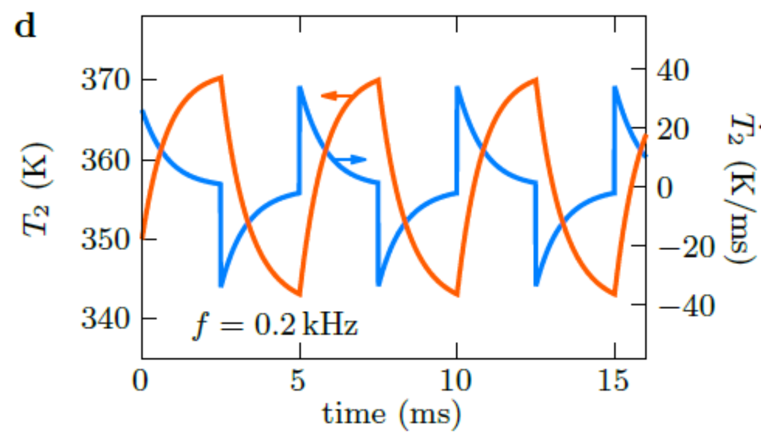

$$c_v\delta\, dT_2/dt = \mathcal{P}_r(V_{gi};T_2,t)$$

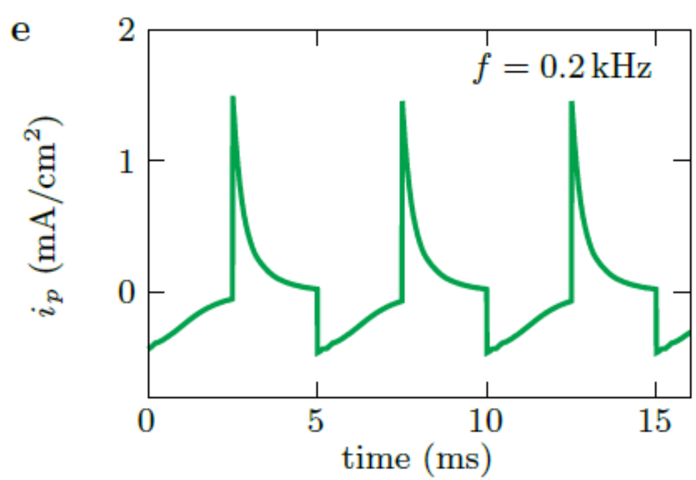

$i_p = p(T_2)\, dT_2/dt$ with p= $\frac{dP}{dT}$ (pyroelectric coeff.)

Performances of converter under SECE cycles

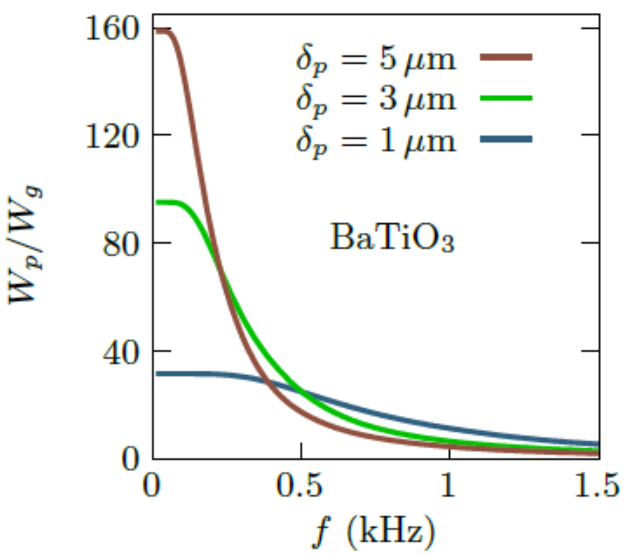

Autonomous (self-powered) converter

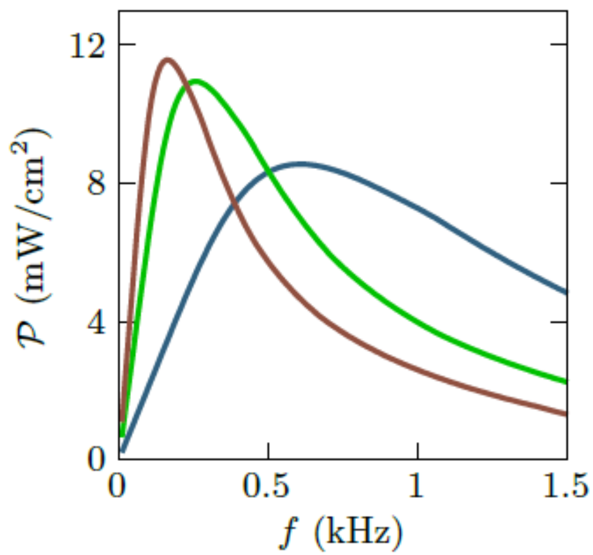

Orders of magnitude larger than NTPV devices

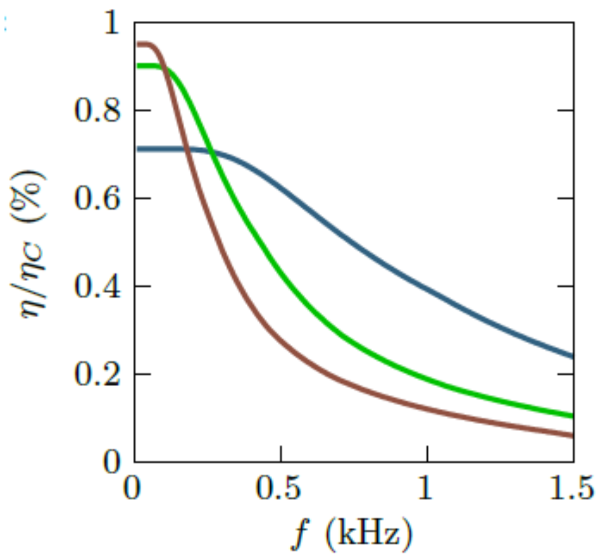

Comparable with others pyro devices

Ericsson cycles can be used to improve these performances

Acknowledgments

Collaborators

S.A. Biehs
(Oldenburg, Germany)

J. C. Cuevas
(Madrid, Spain)

R. Messina
(Palaiseau, France)

A. Rodriguez
(Princeton, USA)

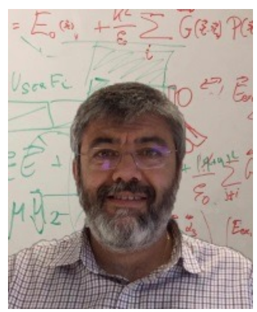

A. Garcia-Martin
(Madrid, Spain)

PhD/Post-Doc students

A. Ott
(Oldenburg, Germany)

I. Latella
(Palaiseau, France)

Thank you!